Concentration and Position-Based Hybrid Modulation Scheme for Molecular Communications

Mustafa Can Gursoy*, Daewon Seo†, and Urbashi Mitra*

*Department of Electrical and Computer Engineering, University of Southern California, Los Angeles, CA, USA
†Department of Electrical and Computer Engineering, University of Wisconsin-Madison, Madison, WI, USA

E-mail: {mgursoy, ubli}@usc.edu, dseo24@wisc.edu

Abstract—Modulation design is a particularly interesting problem in the context of molecular communication via diffusion (MCvD), due to the heavy and signal dependent inter-symbol interference (ISI) imposed on the communication link. To tackle the modulation design issue in MCvD, a hybrid modulation family is proposed in this study. The proposed scheme operates by combining conventional concentration constellations with pulse position modulation symbols, and is able to encode more bits into a single joint symbol than traditional concentration or position-based schemes. Called molecular concentration-position modulation (MCPM), it is shown through theoretical and numerical results that the proposed scheme yields promising error performances, especially in the regime with high ISI and low transmission power. Furthermore, MCPM only utilizes a single type of molecule, which suggests an easier implementability for micro- or nano-scale machinery.

Index Terms—molecular communications, Brownian motion, hybrid modulation, molecular concentration-position modulation.

I. INTRODUCTION

Molecular communication via diffusion (MCvD) is a way of establishing communication links using the diffusive nature of molecules [1], mainly for its promising use in nanonetworks [2]. Achieving MCvD links can be established by encoding information within different physical properties of molecular signals, including but not limited to their quantity [3], type [4], temporal position [5].

After their emission from the transmitter, the emitted molecules exhibit Brownian motion, which results in their arrival times at the receiver end to be probabilistic [6]. This stochastic nature of molecule arrivals causes inter-symbol interference (ISI) and signal-dependent noise [7]. ISI is a major issue against achieving high data rate MCvD systems, as it hinders reliable communication as time intervals between consecutive emissions become shorter.

Several studies show that if the MCvD system has access to multiple types of molecules, hybrid concentration-type modulations, which can alleviate the ISI and noise issues, can be constructed. These works mainly rely on clever utilization of the available molecule types to mitigate the effect of ISI on a concentration-based modulation. Among these studies, [8] and [9] utilize multiple types of available molecules to transmit independent parallel streams of concentration shift

This research has been funded in part by one or more of the following grants: ONR N00014-15-1-2550, NSF CCF-1718560, NSF CCF-1410009, NSF CPS-1446901, NSF CCF-1817200, and ARO 74745LSMUR.

keying (CSK, [3]) symbols, in order to increase the achievable information rate. In [10], the idea of parallel CSK streams is further advanced by emitting inhibitory molecules, alongside the information molecules, to further reduce ISI. A dualmolecule modulation scheme is proposed in [11], where the type of molecule used in CSK is changed according to whether the next bit to be transmitted is a bit-1 or bit-0. Similarly, the idea of modulating according to the run-lengths within the information bit string is considered in [12], where one molecule type carries the bit information while the other conveys the run-length of the said bit. Mentioned multipletype molecule hybrid modulation techniques are shown to increase communication performance compared to standard concentration and type modulations. That being said, it is also worth mentioning that these schemes require the micro- or nano-scale machinery to be able to synthesize, store, and sense multiple types of molecules, which necessitates higher device complexity and may limit their physical implementations.

Encoding information within the temporal release of emissions is considered in several studies in the context of molecular communications. Among these studies, works such as [13]– [16] consider molecular timing channels (MTC), with a goal of discussing fundamental limits of an MTC without confining the modulation scheme to have a discrete symbol set. Over one-shot communication systems on MTCs (i.e. without ISI consideration), [17] considers the well-known pulse-position modulation (PPM) with a finite set of constellation points, and derives its optimal detector. Noting the computational complexity and probable detection delay associated with the optimal detector, [18] proposes several sub-optimal detectors for the scheme. The binary version of PPM is introduced to the field of molecular communications by [5], which demonstrates the scheme to be outperformed by CSK. Recently, it is found by [19] that utilizing higher order PPM in MCvD in ISI-heavy channels improves error performance, courtesy of its sparse transmission strategy.

In this study, inspired by the hybrid modulation concept and the findings of [19] that suggest the benefits of using higher order PPM in MCvD, we propose a hybrid MCvD modulation scheme that utilizes a single type of molecule. The proposed scheme combines PPM constellations with conventional CSK symbols and is called the molecular concentration-position modulation (MCPM). We find that the selection of concentration constellations in MCPM poses a trade-off between errors

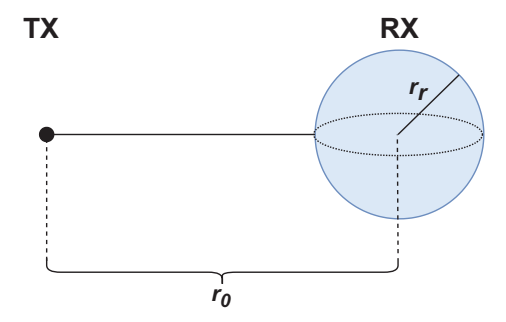


Fig. 1. The considered system model.

in detecting concentration or position-based constellations, suggesting an optimization problem on the emission intensity difference of the concentration constellations while keeping the average number of emitted molecules constant. Through error analysis and computer simulations, we find that with proper selection of the concentration constellations, the proposed scheme can enhance the error performance of an MCvD system. Our numerical results show that the proposed scheme outperforms the existing schemes when the received signal quality is low (i.e. in the high ISI and low transmission power regime), which suggests its possible use in harsher MCvD channels. Overall, we believe the presented approach can act as a step towards further hybrid modulation design while still conserving the implementational simplicity of single-type molecule MCvD systems.

Rest of the paper is organized as follows: Section II describes the system topology and arrival model utilized in the paper; Section III introduces the proposed hybrid modulation scheme; Section IV presents the theoretical error analysis of the proposed scheme; Section V illustrates the error performance of the proposed scheme comparatively with existing modulation schemes; and Section VI concludes the paper.

II. SYSTEM MODEL

In this paper, we consider an MCvD link between a single point transmitter (TX) and a single synchronized, spherical, and absorbing receiver (RX) in an unbounded, driftless 3-D environment. Throughout the paper, r_0 denotes the point-to-center distance between the TX and the spherical RX, r_r represents the radius of the receiver, and D denotes the diffusion coefficient of the utilized carrier molecule. Overall, Fig. 1 illustrates the considered communication system.

For the system model described by Fig. 1, [20] gives a molecule's arrival probability density with respect to time, denoted by $f_{\rm hit}(t)$, as

$$f_{\rm hit}(t) = \frac{r_r}{r_0} \frac{1}{\sqrt{4\pi Dt}} \frac{r_0 - r_r}{t} e^{-\frac{(r_0 - r_r)^2}{4Dt}}.$$
 (1)

Due to its definition, integrating (1) with respect to time yields a molecule's probability of being absorbed by the receiver between its release at t=0 and time t. This cumulative probability is denoted by $f_{hit}(t)$, and is obtained by

$$f_{\rm hit}(t) = \frac{r_r}{r_0} {\rm erfc} \left(\frac{r_0 - r_r}{\sqrt{4Dt}} \right),$$
 (2)

where $\operatorname{erfc}(\cdot)$ represents the complementary error function and is calculated as $\operatorname{erfc}(x) = \frac{2}{\sqrt{\pi}} \int_x^\infty e^{-t^2} dt$. Considering a time slotted MCvD system with a slot dura-

Considering a time slotted MCvD system with a slot duration of t_s , the differences between the consecutive samples of $f_{\rm hit}(t)$ at integer multiples of t_s yield the channel coefficients of the MCvD system. Denoting the n^{th} channel coefficient as h_n , the coefficients can be expressed as

$$h_n = F_{hit}(nt_s) - F_{hit}((n-1)t_s), \quad n = 1, 2, 3, \dots$$
 (3)

Due to the heavy right tail of (1), the channel has infinite memory. However, for practical purposes, a finite channel memory that captures the significant portion of the right tail satisfactorily represents the channel [21]. The channel memory is denoted as L in this paper.

When emitting multiple molecules, the considered system in this paper is modeled by the LTI-Poisson channel [22]. Denoting R_z as the number of molecules that arrive at the receiver in the z^{th} slot, the arrival counts are Poisson distributed as

$$R_z \sim \mathcal{P}\bigg(\sum_{n=1}^L M_{z-n+1}^{TX} h_n\bigg),\tag{4}$$

where M^{TX} denotes the number of emitted molecules in the beginning of a symbol duration, and $\mathcal{P}(\cdot)$ represents the Poisson distribution.

III. PROPOSED SCHEME

The proposed scheme merges the conventional binary CSK (BCSK) with PPM constellations to construct a single-type molecule hybrid modulation scheme. At the transmitter side, the bit sequence ${\bf u}$ is arranged in groups of $1+\log_2 {\cal K}$ bits, where ${\cal K}$ is the PPM order that is to be employed. The first $\log_2 {\cal K}$ bits determine the position-based constellation, which is the release sub-interval of the emitted molecules. After the selection of the temporal position of the molecule emission, the last bit in the group decides on the BCSK symbol to also modulate the intensity of the transmitted signal, resulting in a concentration-position joint symbol. Stemming from its components, the scheme is called ${\cal K}$ -ary molecular concentration-position modulation (${\cal K}$ -MCPM), where the parameter ${\cal K}$ defines the utilized ${\cal K}$ -ary PPM.

In order to provide a fair comparison among the error performances of MCvD schemes, different schemes are analyzed under the same bit rate $(\frac{1}{t_b})$ and average number of emitted molecules per bit (M) [19], [23]. While adopting the average emitted molecules per bit (M) and the communication bit rate $(\frac{1}{t_b})$ normalizations, \mathcal{K} -MCPM is able to emit its symbols with a symbol duration of $t_{sym} = (1 + \log_2 \mathcal{K})t_b$ and with $(1 + \log_2 \mathcal{K})M$ molecules on average. Note that t_{sym} denotes the total duration of a single joint MCPM symbol. Recalling

TABLE I
SLOT DURATIONS AND AVERAGE EMITTED MOLECULES PER SYMBOL FOR SINGLE-TYPE MOLECULE MCVD SCHEMES

Modulation Scheme	BCSK	2 -PPM	4 -PPM	8 -PPM	2-MCPM	4-MCPM	8-MCPM
Transmitted bits	1	1	2	3	2	3	4
per unit symbol	·	1			2	3	
Sub-intervals	1	2	4	8	2	4	8
per symbol							
Sub-interval duration (t_s)	t_b	$\frac{1}{2}t_b$	$\frac{2}{4}t_b$	$\frac{3}{8}t_b$	$\frac{2}{2}t_b = t_b$	$\frac{3}{4}t_b$	$\frac{4}{8}t_b$
Bit duration	t_b	t_b	t_b	t_b	t_b	t_b	t_b
					BCSK bit-1	BCSK bit-1	BCSK bit-1
Molecules per symbol	2M for bit-1,	M	2M	3M	$2M \times 2\alpha$	$3M \times 2\alpha$	$4M \times 2\alpha$
(M^{TX})	0 for bit-0				BCSK bit-0	BCSK bit-0	BCSK bit-0
					$2M \times 2(1-\alpha)$	$3M \times 2(1-\alpha)$	$4M \times 2(1-\alpha)$
Molecules per bit (on average)	M	M	M	M	M	M	M

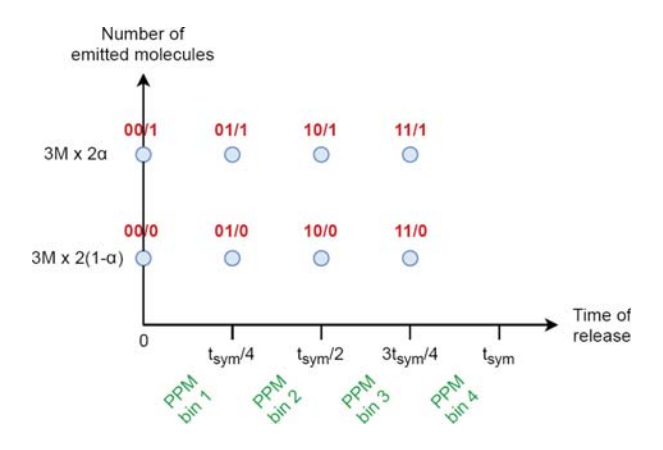


Fig. 2. Transmission strategy of 4-MCPM. First two bits determine the emission time of molecular signal, whilst the third and last bit determines the emission intensity of the signal.

the notation in (3), the bin (sub-interval) durations of the utilized position constellations can be denoted as t_s , which leads to $t_{sym} = \mathcal{K}t_s$.

Noting the aforementioned constraints and assuming equiprobable bit-0 and bit-1 transmissions, the concentration difference between the bit-0 and bit-1 of the BCSK constellation in an MCPM scheme is a design problem. When emitting the molecules with $2\alpha(1+\log_2 \mathcal{K})M$ and $2(1-\alpha)(1+\log_2 \mathcal{K})M$ $\log_2 \mathcal{K})M$ for bit-1 and bit-0, respectively, the value of α needs to be optimized within the region $(\alpha \in [0.5, 1])$ to ensure the system emits $(1 + \log_2 \mathcal{K})M$ molecules on average. Note that if one were to select an α close to 0.5, the concentration constellations become very close to one another, which makes them harder to detect at the RX end. On the other hand, an α value close to 1 would make it difficult for the RX to detect the PPM symbols, since if the bit that modulates BCSK is zero, close to zero molecules are emitted to the channel. In order to demonstrate the proposed scheme, the transmission strategy of an exemplary MCPM scheme is presented in Fig. 2. In addition, Table I presents the average emitted number of molecules per symbol and the for different orders of MCPM, alongside conventional PPM and BCSK.

In order to detect the concentration-position joint symbols of the MCPM scheme, the detectors on the PPM and BCSK

components of the scheme are employed in a consecutive manner. The overall MCPM detector that is utilized in this paper detects the i^{th} joint concentration-position symbol, denoted by s_i , in two steps:

1) The first step is to detect the PPM constellation based on the largest molecule count among the PPM bin intervals using an $\arg\max$ operation on the appropriate subintervals. On the i^{th} concentration-position joint symbol, the maximum count detector can obtain the detected PPM constellation, \hat{j}_i , by performing

$$\hat{j}_i = \arg \max_{j \in \{(i-1)\mathcal{K}+1,\dots,i\mathcal{K}\}} R_j.$$
 (5)

Note that this step is motivated from the assumption that h_1 is the largest channel coefficient.

2) Considering the \hat{j}_i^{th} sub-interval yields the detected PPM component of \hat{s}_i , the MCPM detector performs a fixed threshold detector on the arrival count at the \hat{j}_i^{th} sub-interval to detect the concentration symbol. Denoting the hypotheses corresponding to \hat{s}_i 's BCSK component being a bit-1 or a bit-0 as H_1 and H_0 , respsectively, the MCPM detector obtains the concentration symbol by comparing it to a threshold γ as

$$R_{\hat{j}} \stackrel{H_1}{\gtrless} \gamma. \tag{6}$$

Note that the presented detector is memoryless, as it only considers the $\mathcal K$ sub-intervals of the joint MCPM symbol it detects.

IV. ERROR ANALYSIS

Due to the fact that the ISI and arrival variance of an MCvD system are dependent on past symbols [7], the probability of error can be expressed as an average of error probabilities conditioned on each possible MCPM symbol sequence. Here, we take an approach similar to that of [24] to come up with the theoretical bit error rate (BER). Considering a joint symbol memory of L_s , the error probability is expressed as

$$P_e = \sum_{\forall s_{k-L+1:k}} \left(\frac{1}{|\mathcal{S}|} \right)^{L_s} P_{e|s_{k-L_s+1:k}}, \tag{7}$$

where $s_{k-L_s+1:k}$ denotes a certain MCPM joint symbol sequence between $(k-L_s+1)^{th}$ and k^{th} transmissions, and $|\mathcal{S}|$

represents the cardinality of the joint symbol set. Conditioned on a certain MCPM symbol sequence, $P_{e|s_{k-L_s+1:k}}$ can be found by calculating the expression

$$P_{e|s_{k-L_s+1:k}} = \sum_{n=1}^{|\mathcal{S}|} \frac{d_H(\mathbf{v}_{s_k}, \mathbf{v}_n)}{\log_2(\mathcal{K}+1)} P(\hat{s}_k = n | s_{k-L_s+1:k}), \quad (8)$$

where $d_H(\cdot)$ is the Hamming distance operator between its argument binary vectors, $P(\hat{s}_k = n)$ represents the probability of detecting the MCPM symbol n, and \mathbf{v}_{s_k} and \mathbf{v}_n represent the bit strings associated with s_k and the n^{th} joint MCPM symbols, respectively. Note that (8) computes the average Hamming distance between the n^{th} binary sequence and the sequence that corresponds to s_k , over the probability mass function of the detection of all possible MCPM symbols. Denoting $P(\hat{s}_k = n|s_{k-L_s+1:k})$ as $P(\hat{n})$, characterizing $P(\hat{n})$ is the last required part to complete the derivation. $P(\hat{n})$ can be piecewise expressed as

$$P(\hat{n}) = \begin{cases} P(R_{b_k} > \max(R'_{b_k}), R_{b_k} > \gamma) & v_n[\log_2 |\mathcal{S}|] = 1, \\ P(R_{b_k} > \max(R'_{b_k}), R_{b_k} \le \gamma) & v_n[\log_2 |\mathcal{S}|] = 0, \end{cases}$$

depending on the last bit of n, which selects the concentration constellation and is denoted by $v_n[\log_2 |\mathcal{S}|]$. Here, $b_k \in \{b_1, \dots, b_{\mathcal{K}}\}$ is the decimal representation of the first $\log_2 \mathcal{K}$ bits of \mathbf{v}_n (i.e. the decimal representation of the position constellation). Note that due to its definition, R_{b_k} represents the arrival count corresponding to the slot $R_{(i-1)\mathcal{K}+b_k}$, which is the b_k^{th} sub-interval/bin of the i^{th} MCPM symbol. $R_{b_k}^{'}$ denotes the arrival counts in each PPM bin other than b_k of the i^{th} MCPM symbol. Note that R_{b_k} and $R_{b_k}^{'}$ are conditional random variables (RVs), conditioned on the evaluated $s_{k-L_s+1:k}$ sequence.

Without loss of generality, we select $b_k = b_1$ to exemplify the further steps of the derivation. First, we define a new RV, $Y = \max(R_{b_2}, \dots, R_{b_K})$, to denote the maximum of all arrivals other than R_{b_1} , conditioned on the evaluated $s_{k-L_s+1:k}$. Using the Gaussian approximation on the Poisson arrival counts [25], R_{b_2}, \dots, R_{b_K} are modeled as independent and non-identically distributed Gaussian RVs. Thus, the cumulative distribution function (CDF) of Y, denoted by $F_Y(y)$, can be expressed as

$$F_{Y}(y) = P\left(\max(R_{b_{2}}, \dots, R_{b_{K}}) \leq y\right)$$

$$= \prod_{k=2}^{K} P(R_{b_{k}} \leq y)$$

$$= \prod_{k=2}^{K} \left[1 - Q\left(\frac{y - \mu_{R_{b_{k}}}}{\sigma_{R_{b_{k}}}}\right)\right],$$
(10)

where $Q(\cdot)$ is the well-known Q-function. Note that since arrival counts are assumed to be Poisson distributed RVs in (4), the Gaussian approximation considers both the mean and variance to be $\sum_{n=1}^L M_{z-n+1}^{TX} h_n$ for the z^{th} time slot.

At this point, we denote the probability density function (PDF) of Y as $f_Y(y)$ for further use. To proceed, the derivation

of (9) needs to be separately analyzed for $v_n[\log_2 |\mathcal{S}|] = 0$ and $v_n[\log_2 |\mathcal{S}|] = 1$.

1) For $v_n[\log_2(|\mathcal{S}|)] = 0$, $P(\hat{n})$ can be found by

$$P(\hat{n}) = P(R_{b_1} > \max(R_{b_2}, \dots, R_{b_K}), R_{b_1} \leq \gamma)$$

$$= P(\max(R_{b_2}, \dots, R_{b_K}) < R_{b_1} \leq \gamma)$$

$$= P(Y < R_{b_1} \leq \gamma)$$

$$= \int_{-\infty}^{\gamma} \left[\int_{y}^{\gamma} f_{R_{b_1}}(r) dr \right] f_Y(y) dy$$

$$= \int_{-\infty}^{\gamma} \left[\int_{-\infty}^{r} f_Y(y) dy \right] f_{R_{b_1}}(r) dr$$

$$= \int_{-\infty}^{\gamma} F_Y(r) f_{R_{b_1}}(r) dr,$$
(11)

where $f_{R_{b_1}}(r)$ is the Gaussian PDF with mean $\mu_{R_{b_1}}$ and variance $\sigma_{R_{b_1}}^2$.

2) For the second case where $v_n[\log_2(|\mathcal{S}|)] = 1$, $P(\hat{n}) = P(R_{b_1} > \max(R_{b_2}, \dots, R_{b_K}), R_{b_1} > \gamma)$ can be evaluated over two cases of Y, on whether or not it is greater than γ . Mathematically,

$$P(\hat{n}) = P(R_{b_1} > \max(R_{b_2}, \dots, R_{b_K}), R_{b_1} > \gamma)$$

$$= P(R_{b_1} > Y, R_{b_1} > \gamma)$$

$$= P(R_{b_1} > Y, Y > \gamma) + P(R_{b_1} > \gamma, Y \le \gamma).$$
(12)

The evaluation of $P(R_{b_1} > Y, Y > \gamma)$ is similar to that of (11), and is found by

$$P(R_{b_1} > Y, Y > \gamma) = P(\gamma < Y \le R_{b_1})$$

$$= \int_{\gamma}^{\infty} \left[\int_{y}^{\infty} f_{R_{b_1}}(r) dr \right] f_Y(y) dy$$

$$= \int_{\gamma}^{\infty} \left[\int_{\gamma}^{r} f_Y(y) dy \right] f_{R_{b_1}}(r) dr$$

$$= \int_{\gamma}^{\infty} \left[F_Y(r) - F_Y(\gamma) \right] f_{R_{b_1}}(r) dr.$$
(13)

The evaluation of $P(R_{b_1} > \gamma, Y \leq \gamma)$ can be obtained as

$$P(R_{b_1} > \gamma, Y \le \gamma) = \int_{-\infty}^{\gamma} \left[\int_{\gamma}^{\infty} f_{R_{b_1}}(r) dr \right] f_Y(y) dy$$
$$= \int_{-\infty}^{\gamma} f_Y(y) dy \int_{\gamma}^{\infty} f_{R_{b_1}}(r) dr$$
$$= \int_{\gamma}^{\infty} F_Y(\gamma) f_{R_{b_1}}(r) dr.$$
(14)

Lastly, summing (13) and (14) yields the resultant expression

$$P(\hat{n}) = P(R_{b_1} > \max(R_{b_2}, \dots, R_{b_K}), R_{b_1} > \gamma)$$

$$= \int_{-\infty}^{\infty} F_Y(r) f_{R_{b_1}}(r) dr.$$
(15)

Note that after the evaluation of Eqs. (9)-(15) for all |S| of the MCPM symbols, the probability mass function of $P(\hat{s}_k = n)$

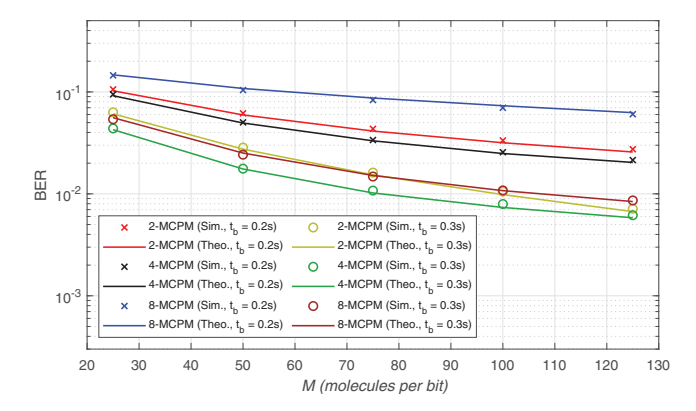


Fig. 3. BER vs. M curves. $t_b=0.2$ and 0.3s, $r_0=10\mu \rm m,~r_r=5\mu m,~D=79.4\frac{\mu m^2}{s}$, and L=12.

is obtained. The rest of the derivation follows by plugging $P(\hat{s}_k = n)$ into (8), and concludes by plugging (8) into (7).

In order to demonstrate the accuracy of the error analysis, Fig. 3 is presented. The results of Fig. 3 suggest that the obtained expression follows the Monte Carlo simulated BER closely, which is expected since the presented approach aims to yield the exact BER, rather than providing a bound. However, slight discrepancies between simulated and analytical curves are indeed present, which are mainly due to the approximation error of the Poisson arrival counts with Gaussian RVs.

V. NUMERICAL RESULTS

A. Error Probability vs. Number of Emitted Molecules

In this section, the error performance of the proposed MCPM scheme is presented comparative to its concentration-(BCSK) and position-based (PPM) components, through computer simulations. Please note that considering the presented scheme can be implemented with only a single type of molecule, comparisons with schemes such as the molecule shift keying [3] or the hybrid schemes presented in [8]–[12] are omitted in order to have fairness in device complexity, emphasizing that these schemes require more complex nanoscale machinery that can synthesize and sense multiple types of molecules.

When comparing the evaluated schemes, BCSK is demodulated using a fixed threshold detector similar to the one utilized in (6), and the PPM symbols are demodulated using the maximum count detector similar to (5). All α values of the MCPM schemes are numerically optimized using exhaustive search between 0.5 and 1 with 0.01 incremental steps. The concentration symbol detectors of both MCPM and CSK are implemented using their optimal γ threshold values. Figs. 4 and 5 present the BER vs. M curves corresponding to BCSK, different orders of MCPM, and PPM schemes for two different bit durations. Please note that for the MCvD with parameters as considered in these figures, a bit duration of $t_b = 0.2$ s corresponds to a relatively high ISI scenario, whilst $t_b = 0.3$ s corresponds to a friendlier channel due to its lower ISI imposition.

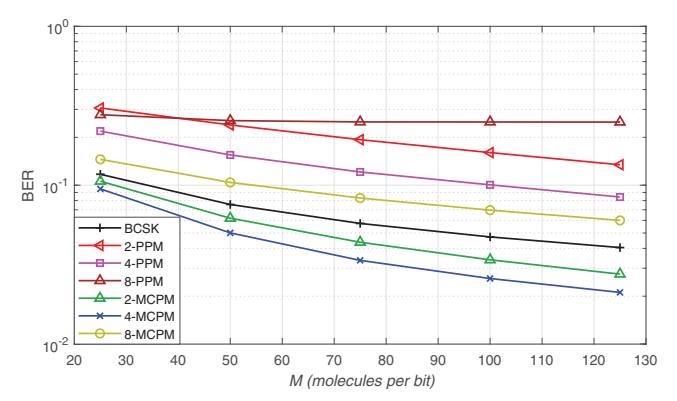


Fig. 4. BER vs. M curves. $t_b=0.2$ s, $r_0=10\mu\text{m},\ r_r=5\mu\text{m},\ D=79.4\,\frac{\mu m^2}{}$, and L=12.

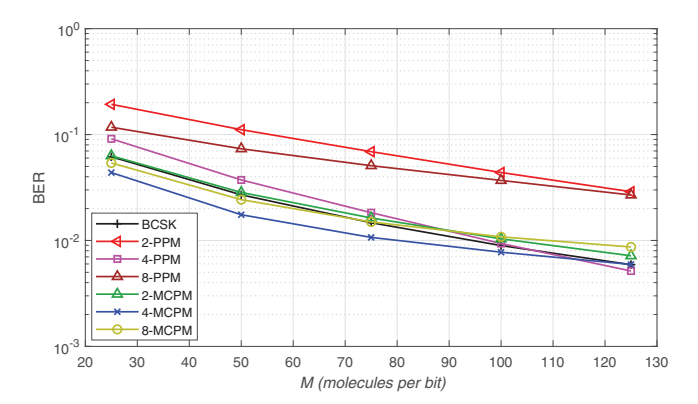


Fig. 5. BER vs. M curves. $t_b=0.3$ s, $r_0=10\mu{\rm m},~r_r=5\mu{\rm m},~D=79.4\frac{\mu m^2}{c}$, and L=12.

The results of Figs. 4 and 5 suggest that one or more MCPM schemes outperform BCSK and PPM schemes for the evaluated scenarios. This performance enhancement can be attributed to: i) the increased and tunable (through the selection of α) degree of freedom the MCPM provides over its components, ii) the fact that it can emit its symbols with a larger symbol duration and average number of molecules while still satisfying the bit rate and transmission power constraints shown in Table I. It can be observed that among the MCPM schemes, 4-MCPM is found to yield the lowest BER results for the evaluated scenarios.

B. Error Probability vs. Bit Rate

Noting from the results of Figs. 4 and 5 that the amount of ISI that is faced by the MCvD schemes directly affect their communication performance, BER vs. t_b curves of the evaluated schemes are demonstrated in Fig. 6. In order to generate the figure, a total time $t_{\rm total}$ that is arbitrarily large and sufficiently captures the right tail of (1) is considered, and each ISI window length L is calculated according to the considered t_b value. This procedure is done to impose all data points to a similar total ISI. Note that if one were to choose a fixed L value, the considered total ISI at $t_b = 0.1$ s would

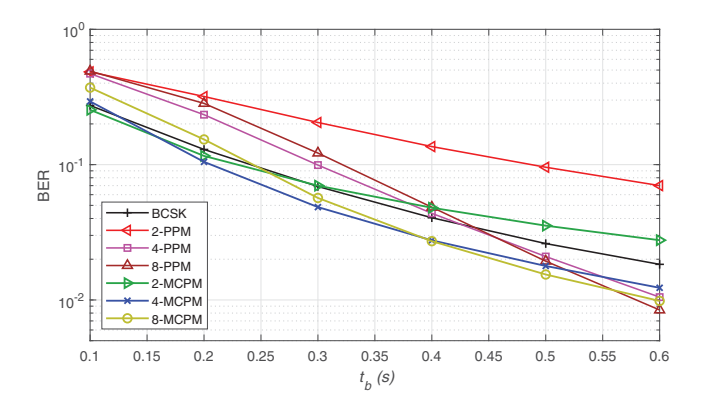


Fig. 6. BER vs. t_b curves. M=25 molecules, $r_0=10\mu\text{m},~r_r=5\mu\text{m},~D=79.4\frac{\mu m^2}{s}$, and $t_{\text{total}}=15\text{s}$.

be considerably lower than $t_b = 0.6$ s, and would model the system for $t_b = 0.1$ s over-optimistically.

The results of Fig. 6 show that at the higher data rate regime, MCPM schemes (specifically 4-MCPM) outperform the other evaluated schemes. However, it should be noted that the PPM schemes provide better slopes as t_b increases, which can also be verified from the results of Fig. 5. Overall, the aggregate inference from Figs. 4-6 is that MCPM provides a promising scheme to an MCvD system that utilizes a single type of molecule, especially when: i) the number of emitted molecules are small, ii) the ISI the system faces is high. Together, this regime can be considered to correspond to the low signal-to-interference and noise ratio (SINR) regime [26].

VI. CONCLUSION

In this paper, a single-type molecule hybrid modulation scheme for molecular communication via diffusion systems has been presented. Through analytical and numerical results, it has been shown that especially in the low SINR regime, the presented modulation family is capable of yielding promising results, while still using conventional and memoryless detectors at the receiver end. The consideration of memory-aided and more sophisticated receivers, theoretical cost functions that can be used to optimize the tunable parameter α , and robustness to mis-synchronization issues are considered as future works.

REFERENCES

- N. Farsad, H. B. Yilmaz, A. Eckford, C. B. Chae, and W. Guo, "A comprehensive survey of recent advancements in molecular communication," *IEEE Commun. Surveys Tutor.*, vol. 18, no. 3, pp. 1887–1919, Feb. 2016.
- [2] I. F. Akyildiz, F. Brunetti, and C. Blázquez, "Nanonetworks: A new communication paradigm," *Elsevier Comput. Netw.*, vol. 52, no. 12, pp. 2260–2279, Aug. 2008.
- [3] M. S. Kuran, H. B. Yilmaz, T. Tugcu, and I. F. Akyildiz, "Modulation techniques for communication via diffusion in nanonetworks," in *Proc. IEEE Int. Conf. Commun. (ICC)*, Apr. 2011, pp. 1–5.
- [4] N.-R. Kim and C.-B. Chae, "Novel modulation techniques using isomers as messenger molecules for nano communication networks via diffusion," *IEEE J. Sel. Areas Commun.*, vol. 31, no. 12, pp. 847–856, Jan. 2013.

- [5] N. Garralda, I. Llatser, A. Cabellos-Aparicio, E. Alarcón, and M. Pierobon, "Diffusion-based physical channel identification in molecular nanonetworks," *Nano Commun. Netw.*, vol. 2, no. 4, pp. 196–204, Dec. 2011.
- [6] K. V. Srinivas, A. W. Eckford, and R. S. Adve, "Molecular communication in fluid media: The additive inverse Gaussian noise channel," *IEEE Trans. Info. Theory*, vol. 58, no. 7, pp. 4678–4692, July 2012.
- [7] D. Kilinc and O. B. Akan, "Receiver design for molecular communication," *IEEE J. Sel. Areas Commun.*, vol. 31, no. 12, pp. 705–714, Dec. 2013.
- [8] H. Arjmandi, A. Gohari, M. N. Kenari, and F. Bateni, "Diffusion-based nanonetworking: A new modulation technique and performance analysis," *IEEE Commun. Lett.*, vol. 17, no. 4, pp. 645–648, Mar. 2013.
- [9] M. H. Kabir, S. M. R. Islam, and K. S. Kwak, "D-MoSK modulation in molecular communications," *IEEE Trans. Nanobiosci.*, vol. 14, no. 6, pp. 680–683, Sep. 2015.
- [10] S. Pudasaini, S. Shin, and K. S. Kwak, "Robust modulation technique for diffusion-based molecular communication in nanonetworks," arXiv preprint arXiv:1401.3938, 2014.
- [11] B. Tepekule, A. E. Pusane, H. B. Yilmaz, C.-B. Chae, and T. Tugcu, "ISI mitigation techniques in molecular communication," *IEEE Trans. Mol. Biol. Multi-Scale Commun.*, vol. 1, no. 2, pp. 202–216, Jun. 2015.
- [12] S. Pudasaini, S. Shin, and K. S. Kwak, "Run-length aware hybrid modulation scheme for diffusion-based molecular communication," in *Proc. IEEE Int. Symp. on Commun. and Info. Tech. (ISCIT)*, Sept. 2014, pp. 439–442.
- [13] A. W. Eckford, "Nanoscale communication with brownian motion," in Annual Conf. Info. Sci. and Syst. (CISS), Mar. 2007, pp. 160–165.
- [14] H. Li, S. M. Moser, and D. Guo, "Capacity of the memoryless additive inverse gaussian noise channel," *IEEE J. Sel. Areas Commun.*, vol. 32, no. 12, pp. 2315–2329, Dec. 2014.
- [15] C. Rose and I. S. Mian, "Inscribed matter communication: Part I," *IEEE Trans. Mol. Biol. Multi-Scale Commun.*, vol. 2, no. 2, pp. 209–227, Dec. 2016
- [16] —, "Inscribed matter communication: Part II," *IEEE Trans. Mol. Biol. Multi-Scale Commun.*, vol. 2, no. 2, pp. 228–239, Dec. 2016.
- [17] Y. Murin, N. Farsad, M. Chowdhury, and A. Goldsmith, "Optimal detection for one-shot transmission over diffusion-based molecular timing channels," *IEEE Trans. Mol. Biol. Multi-Scale Commun.*, vol. 4, no. 2, pp. 43–60, Jun. 2018.
- [18] ——, "Exploiting diversity in one-shot molecular timing channels via order statistics," *IEEE Trans. Mol. Biol. Multi-Scale Commun.*, vol. 4, no. 1, pp. 14–26, Mar. 2018.
- [19] B. C. Akdeniz, A. E. Pusane, and T. Tugcu, "Position-based modulation in molecular communications," *Nano Commun. Netw.*, vol. 16, pp. 60– 68, Jun. 2018.
- [20] H. B. Yilmaz, A. C. Heren, T. Tugcu, and C.-B. Chae, "Three-dimensional channel characteristics for molecular communications with an absorbing receiver," *IEEE Commun. Lett.*, vol. 18, no. 6, pp. 929–932, Jun. 2014.
- [21] Y. Lu, X. Wang, M. D. Higgins, A. Noel, N. Neophytou, and M. S. Lee-son, "Energy requirements of error correction codes in diffusion-based molecular communication systems," *Nano Commun. Netw.*, vol. 11, pp. 24 35, Mar. 2017.
- [22] G. Aminian, H. Arjmandi, A. Gohari, M. Nasiri-Kenari, and U. Mitra, "Capacity of diffusion-based molecular communication networks over LTI-Poisson channels," *IEEE Trans. Mol. Biol. Multi-Scale Commun.*, vol. 1, no. 2, pp. 188–201, Nov. 2015.
- [23] M. Damrath, H. B. Yilmaz, C.-B. Chae, and P. A. Hoeher, "Array gain analysis in molecular MIMO communications," *IEEE Access*, vol. 6, pp. 61 091–61 102, Oct. 2018.
- [24] M. C. Gursoy, E. Basar, A. E. Pusane, and T. Tugcu, "Index modulation for molecular communication via diffusion systems," *IEEE Trans. Commun.*, vol. 67, no. 5, pp. 3337–3350, May 2019.
- [25] H. B. Yilmaz, C.-B. Chae, B. Tepekule, and A. E. Pusane, "Arrival modeling and error analysis for molecular communication via diffusion with drift," in *Proc. ACM Int. Conf. Nanoscale Comput. and Commun.*, Sep. 2015.
- [26] V. Jamali, A. Ahmadzadeh, and R. Schober, "On the design of matched filters for molecule counting receivers," *IEEE Commun. Lett.*, vol. 21, no. 8, pp. 1711–1714, May 2017.